

SINGLE PHASE LOW VOLTAGE CHARGER FOR ELECTRIC VEHICLES

ER. GAURAV SHARMA & ER. HARKAMAL DEEP SINGH

M.Tech. Electrical Engineering, GGS College of Modern Technology, Mohali, India

Assistant Professor, GGS College of Modern Technology, Mohali, India

ABSTRACT

This Paper Focuses on the Charging of Electric Batteries Using a Single Phase on-Board Unidirectional Charger for Electric Vehicles. Two Ac-Dc Full Bridge Bidirectional Boost Converters (120v Ac to 400v Dc) Plus a Half Bridge Dc-Dc Buck Converter Make Up the Charger. for Charging, Ac to Dc Full Bridge Boost Converters and Dc-Dc Buck Converters have been Created. Single Phase on-Board Unidirectional Charger for Charging Electric Vehicles has been Designed as the Controller for Both Converters. The Purpose of an Ac-Dc Converter Controller is to Override Grid or Utility Active and Reactive Power (P-Q) Commands. The Settings of the Dc Side Can be Modified by Changing The Controllable Commands. A Separate Controller is Supplied for Each Converter to Maintain the Balance Between Input and Output Power. The Ac-Dc Converter Controller Aids in Boost up the Input Grid Voltage to 400v Dc. the Charger Must be Able to Override The Grid's or Utility's Instructions/Commands. The Dc-Dc Converter Converts Constant Voltage to Variable Voltage, Limiting the Amount of Current Necessary To Charge The Battery. The Main Focus of this Manuscript is on the Level-1 and Level-2 on-Board Charging Systems. The EV Charger is Set to Charge-Only Mode, Which Means it Only Delivers Active Power to the Grid. The Charging System for Electric Vehicles has been Modelled, and the Resulting State of Charge (Soc) has been Compared to the three already Developed Charging Systems.

KEYWORDS: *Ac-Dc Boost Converter, Battery Charger, Dc-Dc Buck Converter, Plug-In Electric Vehicle & Unified Controller*

Original Article

Received: May 05, 2022; **Accepted:** May 25, 2022; **Published:** Jun 16, 2022; **Paper Id.:** IJEEERJUN20224

1. INTRODUCTION

Electric vehicles are rapidly expanding in today's environment and will continue to do so in the next years. These cars are the best alternative to traditional Internal Combustion Engine (ICE) automobiles [1]. Rather than a gasoline or diesel engine, electric vehicles are powered by an electric motor. As a result, electric vehicles do not emit pollutants because they do not have a tailpipe. During peak load hours, a large number of electric vehicles cause congestion in the distribution system. To address this issue, coordinated charging will be required to reduce the negative impact on the grid [2], [3].

According to a report, the usage of energy will increase global transportation by 45 percent by 2030. Increased adoption of electric vehicles is required to combat climate change and reduce oil use. However, due to capital expenses, operating costs and a lack of charging infrastructure, there are several limitations to the acceptance of electric cars (EVs). PEV research is still ongoing, with the goal of making significant progress in the near future.

The EV charger illustrated above, on the other hand, is made up of two converters that share a DC link. The charger is a device that connects the grid to the car. These two converters are connected by a DC link. The DC link is critical for charging the battery from the grid to the vehicle. With the help of a charger, power is transformed from AC to DC. The charger's sole purpose is to obey the grid's or utility's/power user's directions. These are the commands which will be discussed further. In recent years, synchronous condensers, capacitor banks, and other devices have been used to compensate for the reactive power consumed by utility grids. Reactive power transfer from source to load incurs significant transmission and distribution losses, and reactive power at the supply end differs from reactive power at the load end. Transmission and distribution losses increase strain on the distribution transformer, causing the voltage profile on the distribution transformer side to drop. It is preferable to generate reactive power close to the load to reduce losses. On-Board chargers are the best option for this because they provide the highest level of efficiency. The PEV charger can also perform power quality operations, such as reactive power adjustment, regulation of voltage, filtering of harmonics & power factor correction [4].

The charger's primary goal is to charge the battery of an electric car by coordinating with the grid. According to studies that show a large number of PEVs connected, charger ratings in those PEVs, distribution transformer rating (25-100kVA), charging current harmonics, and geographic location, the lifetime of a distribution transformer can be reduced to 26% of its normal working life expectancy [5], [6]. The main benefit of a high number of PEVs is that reactive power can be induced close to the load during peak load times. The design of a battery charger is critical for regulating power flow and ensuring that electric power is delivered reliably. Electric Vehicle batteries act as power storage devices to store the power in batteries for a particular interval of time and the stored power can be used when needed [7]. Charger plays an important role to the integration of EVs in the grid so as to demote the negative impact of congestion network of electric vehicles in charging station. The prime cons of EVs are its storage capability. Amid high load times, the EVs feed stored power back to the grid and hence increase the efficiency of the distribution transformer (DT) and also alleviate the overloading of DT [6]. The customers will be given a bonus for that [2], [8-10].

However, the change in P_{cmd} and Q_{cmd} will make changes in dc link voltage and further changes the charging current of battery. In this way, the battery charging is controlled. Reactive power assistance to the grid does not affect to the SOC of the battery but it does make changes in dc-link capacitors because more charging and discharging cycles are used [11].

In [12], [13], [14], and [15], mainly two controllers are utilized for ac-dc and dc-dc converters. The controller utilizes isolate references for AC-DC and DC-DC stages (i.e. P_{cmd} , Q_{cmd} , i_{bt*}). The charger that is used to follow only P_{cmd} and Q_{cmd} is profitable for smart grid applications. The charger proposed in [2] requires large size of the DC-link capacitor, which results in limited reactive power output. In this proposed work, the single phase PEV charger is developed and its block diagram has been presented. The charger consists of two converters and their corresponding controllers. In today's era electric vehicles are in trending position. However, the work done on low voltage supply to electric vehicles is very rare. Therefore, the authors are motivated to develop the pace in this work area so that low voltage applications can be applicable in rural and urban areas at rapid rate. The work on high voltage part has been done in large amount; therefore, there is a need to focus on low voltage side for charging the electric vehicles especially in domestic areas.

The proposed charger and its control strategy is developed in MATLAB SIMULINK. Section II portrays the converter working and its description. Section III is mainly focused on the design and working of controller. Section IV

concentrates on simulation results of the proposed PEV charger.

2. DESCRIPTION OF PROPOSED PEV CHARGERCONVERTER

The charger proposed, has two stages which are AC-DC boostconverter and the DC-DC buck converter as shown in Figure 1. The ac-dc full bridge boost converter is useful to transform low ac voltage (120V) into high dc voltage (400V) without using a transformer. The dc-dc buck converter is used to convert high dc link voltage into low battery voltage and dc-dc controller is also used to regulate the Battery Charging Current [16]. The prime motive of the charger is to charge the electric vehicle via proper coordination between EV and grid. The converters used in the charger consists of corresponding controllers. The ac-dc converter is experienced with bipolar modulation which means converter output is either $+V_{dc}$ or $-V_{dc}$. During the turn-on interval of switches S1 and S4, switches S2 and S3 remains switched off and vice-versa. DC link voltage (V_{dc}) takes part in both ac-dc and dc-dc controllers and hence V_{dc} can be taken as a reference to control the battery charging current (i_{bt}). To obtain dc-dc buck operation switches S5 and D6 are switched on as shown in Figure 1. The charger operates in charging only mode. However, the inductor at grid side (L_{ac}) is habituated to boost up low ac grid voltage to high dc link voltage (V_{dc}) across dc link capacitor. During charging of battery, the presence of MOSFET switches causes large amount of switching losses. Due to this, the charger must have to follow P_{cmd} and Q_{cmd} , so that the input power must be equal to output power without any loss.

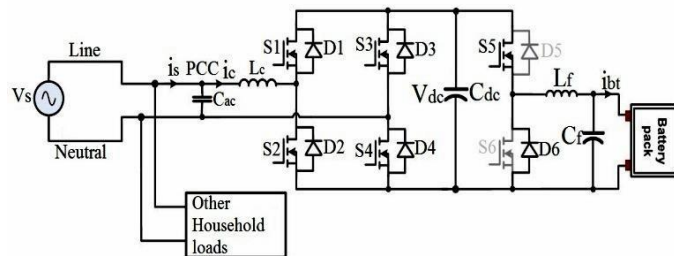


Figure 1: Battery Charger Circuit Diagram.

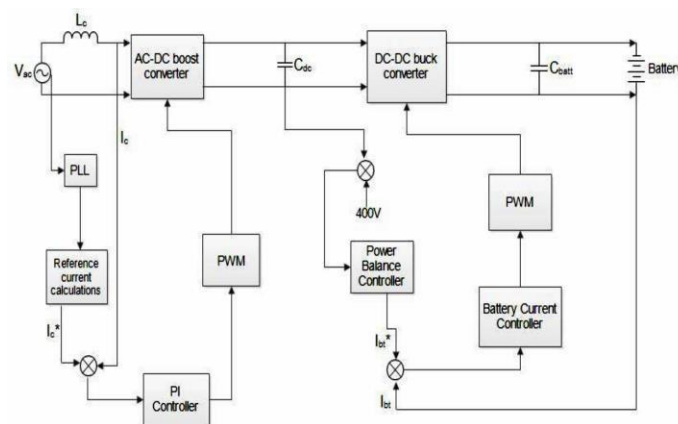


Figure 2: Complete Block Diagram of Proposed Charger.

The lithium-ion battery is considered that operates in both CC and CV charging modes. Figure 2 represents the complete block diagram of a working charger. The charger used here is a unidirectional one and operates in G2V mode only. In general, two types of chargers may be utilized; these include On-board and Off-board chargers. The on-board charger can charge the batteries at any outlet which is available at either home or any workplace. The on-board chargers

have limited power rating because of their limited size and dimensions; therefore, they take more time to charge the batteries [16]. The off-board chargers on the other hand are used for fast charging and take lesser time to charge a vehicle. The on board chargers have drawn more attention because of their low cost, easy availability, good efficiency and ease of use [17].

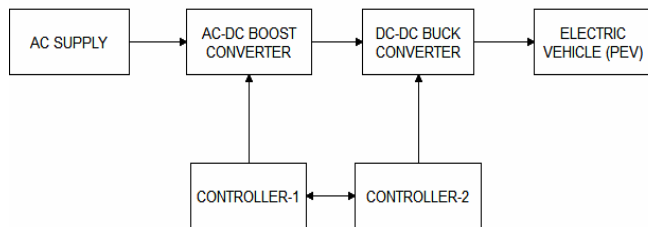


Figure 3: Schematic Block Diagram of Proposed Charger.

Figure 3 shown above represents the schematic block diagram of proposed PEV charger. In this there are total six blocks and each block represents its own function. The supply carried from the grid is of alternating type i.e. ac supply. The supply carried away from grid utility is available at 120V or 230V. The ac supply passes through ac-dc converter and dc-dc converter and further to PEV battery. The PEV battery is a dc type battery which requires dc voltage and dc current. The ac-dc converter is regulated by ac-dc controller and dc-dc converter is regulated by dc-dc controller. After controlling the voltage and current, the power is transferred to electric vehicle battery (EV). The parameters used in 1.44kVA charger are shown in Table I. By using these parameters the required operation can be done.

Table 1: Parameters of 1.44kVA Charger [11]

Parameters	Symbol	Values
Apparent power of the charger	S	1.44×10^3 VA
Supply Voltage	V_a	120 V RMS
Frequency	F	60 Hz
Supply-side inductance	L_c	1.0mH
Switching frequency for ac-dc converter	F_{sw1}	24×10^3 Hz
DC link voltage	V_{dc}	385 V
Switching frequency for dc-dc converter	F_{sw2}	42×10^3 Hz
DC link capacitance	C_{dc}	440×10^{-6} F
Filter capacitor (battery side)	C_f	190 μ F
Filter inductance (battery side)	L_f	390 μ H

3. DESIGN OF PROPOSED PEV CONTROLLER

In this research work, the PEV charger works only in first quadrant of P-Q plane. Therefore, the charger operates just in charging only mode. The G2V power flow is considered positive.

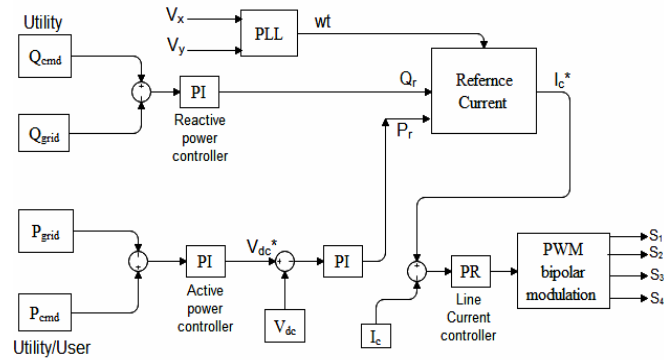


Figure 4: Block Diagram of Controller for AC-DC Converter.

Figure 4 represents the block diagram of ac-dc boost converter. In this the conversion of signals is done through p-q theory. In this theory two voltage and current orthogonal signals are obtained by delay function. After that the output of instantaneous p-q block passes through low pass filters. After that the output P and Q are equated with P_{cmd} and Q_{cmd} provided by user/utility. The delayed (Orthogonal) signals are used for PLL algorithm (Phase locked loop) algorithm that tracks the phase angle of line voltage and induce the reference phase signal for battery charging current. The ac-dc boost converter controls the dc link voltage (V_{dc}). The active power command (P_{cmd}) is used as reference power for purpose of battery charging. The difference between output powers and command powers further passes through two different PI controllers i.e. active and reactive power controllers. The main function of PI controllers is to demote the steady state error. The output of P-loop (V_{dc}^*) is compared with dc link voltage (V_{dc}). The difference between actual and reference signals further passes through dc voltage controller (PI Controller) which produce power called P_r . Q_r in Q loop is produced as same as in case of P-loop. The main function of these two signals is to produce reference charging current (i_c^*). The reference charging current is further compared with actual charging current (i_c). The difference between these two parameters results in an error and this is further sent to PR controller to control the charging current [18]. After this the charging current passes through bipolar modulation. The yield of bipolar modulation results in gate pulses for switches. Hence in this way AC-DC converter controller controls the charging current by applying gate pulses to the switches.

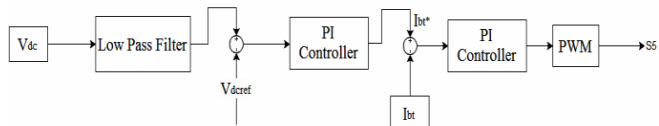


Figure 5: Block Diagram of Controller for DC-DC converter.

Figure 5 represents the block diagram of dc-dc converter. The DC-DC buck converter is used to reduce the dc link voltage to battery voltage so that charging current must flow from high voltage to low voltage i.e. from dc link capacitor to PEV battery. The DC-DC converter must have a controller that controls the above process. In this controller the sensed dc link voltage must proceed through low pass filter that helps to reduce ripples in it. The reference dc link voltage (V_{dc}^*) is equated with sensed dc link voltage (V_{dc}). The difference between actual and reference signals passes through power balance controller (PI controller). The PI controller outputs a reference charging battery current (i_{bt}^*). The sensed battery charging current is equated with reference charging current of battery (i_{bt}^*) [19]. The obtained result is regulated with battery current controller (PI Controller). Pulse Width Modulation (PWM) block receives the output signal of battery

current controller (PI Controller) and generates duty cycle (S_5) consequently.

4. CONTROL METHODOLOGY

A. PI (Proportional Integral) Controller

The Proportional and integral (PI) refers to integration of error signal for a period of time. Error signal is proportional to rate of change of correcting signal. Figure 6 represents the block diagram of PI controller.

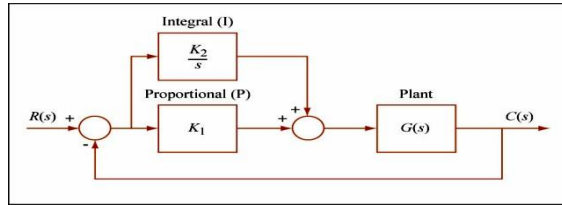


Figure 6: PI Controller Block Diagram.

Transfer function of the PI controller is given as follows:

$$G(s) = K_p + \frac{K_i}{s} \quad (1)$$

Where K_p is the constant of proportionality and K_i is the integral gain of the PI controller. The controller will perform until error is completely removed. The difference between generation and demand will produce error. The steady state error is reduced with the help of PI controller and at the same time reduces the settling time.

The p-q theory is used to calculate P and Q . The 'x' components are indicators of sensed signals. The 'y' signals are produced by delay function. The orthogonal signals (y) are delayed by one-quarter of grid period which is equal to (1/240) corresponds to 100 samples with 24 kHz sampling frequency [20]. The signals are delayed for utilization in PLL algorithm which tracks phase angle of line voltage and produces a reference signal for charging current. The single-phase active is given by:

$$P = 1/2(V_x \times I_x + V_y \times I_y) \quad (2)$$

$$Q = -1/2(V_x \times I_y + V_y \times I_x) \quad (3)$$

There are two low pass filters that are used to yield P and Q outputs. The active power command (P_{cmd}) is given by the client and reactive power command (Q_{cmd}) is provided by utility/grid. The charger must have to follow these power commands for efficient operation. During peak load hours grid can regulate P_{cmd} to harmonize charging power. If any client or costumer provides reactive power to the grid then grid must provide an incentive to the costumer. However, P_{cmd} and Q_{cmd} must be examined before being sent to the charger.

The active power (P) must be matched with active power command (P_{cmd}) to fulfil the desired operation. This can be by changing dc link voltage (V_{dc}^*). The loop equation for this is as follows

$$V_{dc}^* = (K_p^a + \frac{K_i^a}{s}) \times P_{cmd} - P \quad (4)$$

The dc voltage loop (v-loop) follows dc link voltage (V_{dc}^*). The difference of sensed dc link voltage and reference dc link voltage passes through PI controller. The constants of the controller are changed accordingly to match the actual and reference value. This loop's output produces reference tracking active power (P_r). The equation for this is as follows:

$$P_r = (K_p + \frac{K_i}{s}) \times (V^* - V_d) \quad (5)$$

The output Q is matched with Q_{cmd} from the grid with the help of reactive power loop (Q-loop). The mismatch between actual reactive power (Q) and reactive power command (Q_{cmd}) is passed through PI controller whose constants have to be modified to match the sensed and reference reactive power (Q_r).

The equation for Q-loop is as follows:

$$Q_r = (K_p + \frac{K_i}{s}) \times Q_{cmd} - Q \quad (6)$$

Q-loop tells whether the charger can supply or sink the reactive power. The reference charging current is induced by yields of dc voltage loop and reactive power loop. The following equations are also used to calculate reference charging current (i_c^*).

$$\frac{Q_r}{P_r} \phi = \tan^{-1} \quad (7)$$

$$I_c = \frac{P_r}{V_a \cos \phi} \quad (8)$$

And finally

$$i^* = \sqrt{2} I_c \sin(\omega t - \phi) \quad (9)$$

Where I_c is the RMS value of charging current. V_a is the source voltage.

B. PR (Proportional Resonant) controller

The transfer function of PR controller is:

$$G_{PR} = K_p + \frac{2K_r s}{s^2 + \omega_1^2} \quad (10)$$

Where K_p is the proportional gain and ω_1 , K_r are the resonant frequency and gain, respectively. The PR controller provides an infinite gain at resonant frequency and zero phase shift. However, PR controller is used to regulate the mismatch between reference charging current (i_c^*) and sensed charging current (i_c). The difference between two charging currents are fed to PR controller whose constants are changed to match the sensed and reference charging current. The PR

controller used in this charging system provides smoothness in charging of battery as compared to controllers used by other authors. This is the novelty of this work. The PR controller is infinite gain controller especially used for controlling the charging current. Hence this controller brings the novelty in this charging system. The PR controller yield is used to produce duty cycle (d) for anac-dc converter. The equation for i-loop is as follows:

$$d = \left(K_p^d + \frac{2K_a \omega_c s^*}{s^2 + 2\omega_c s + \omega^2} \right) \times (i_c^* - i) \quad (11)$$

For dc-dc converter, the reference dc link voltage (V_{dc}^*) is equated with V_{dc} . The resultant error passes through power balance controller (PI) controller. The constants of PI controller are modified to remove the mismatch between sensed and reference dc link voltage. The output of PI controller yields reference battery current (i_{bt}^*). The equation for this is as follows:

$$i_{bt}^* = (K_p^e + \frac{K_i^e}{s}) \times (V_{dc} - V_{dc ref}) \quad (12)$$

The loop represented above is used to maintain the input-output balance of power. The main purpose of this loop is to fulfil P_{cmd} so as to charge the battery without any loss. The equation for this loop is as follows:

$$d_0 = (K_p^f + K_i^f) \times (i_{bt}^* - i_{bt}) \quad (13)$$

where d_0 is the duty cycle

In this framework, battery charging current is induced by varying the output voltage of ac-dc boost converter. If there is increase in value of P_{cmd} then V_{dc} also increases to a new benchmark and vice-versa. This small change in V_{dc} yields a change in i_{bt} . Second order harmonics present in DC link voltage are filtered using low pass filters whose transfer function is given below

$$H(s) = \frac{k\omega_{c1}^2}{s^2 + 2s\omega_{c1}s + \omega_{c1}^2} \quad (14)$$

where $\omega_{c1} = 2\pi f_c$, $f_c = 20\text{Hz}$ and $k = \sqrt{2}$.

Table II represents the values of parameters of controller used in above equations. By using these parameters, the battery charging current can be controlled

Table 2: List of Controller Parameters [11]

Parameters	Symbol	Value
Angular frequency	ω	377 rad/s
Crossover angular frequency	ω_c	3.1 rad/s
Proportional const. for current loop (I loop) controller (P-R)	K_p^d	1.2
Integral constant for current loop (i-loop) controller (P-R)	K_i^d	1000

Proportional const. for dc voltage loop (v-loop) controller (PI)	K^b_p	1.5
Integral constant for dc voltage loop (v-loop) controller (PI)	K^b_i	100
Proportional const. for reactive power loop (Q-loop) controller (PI)	K^c_p	0.2
Integral constant for reactive power loop (Q-loop) controller (PI)	K^c_i	30
Proportional const. for active power loop (P-loop) controller (PI)	K^a_p	1
Integral const. for active power loop (P-loop) PI contr.	K^a_i	20
Proportional constant for balance loop controller (PI)	K^e_p	0.045
Integral constant for balance loop controller (PI)	K^e_i	0.5
Proportional constant for battery current (i_{bt}) loop controller (PI)	K^f_p	0.15
Integral constant for battery current (i_{bt}) loop controller (PI)	K^f_i	10

The parameters for 6.6kVA charger is shown in Table III. These values are most suitable for making 6.6kVA charger.

Table 3: Parameters of 6.6kva Charger [21]

Parameters	Symbol	Values
Apparent power of the charger	S	6.6×10^3 VA
Supply Voltage	V_a	230 V RMS
Frequency	F	60 Hz
Supply-side inductance	L_c	1.5mH
Switching frequency for ac-dc converter	F_{swl}	24×10^3 Hz

5. SIMULATION RESULTS OF PROPOSED ELECTRIC VEHICLE CHARGER

The results obtained from the simulation of single phase PEV charger are represented in Figure 7-14. There are two types of chargers used for the charging of electric vehicle battery.

1.44kVA Charger

As explained above the charger works in charging only mode. The G2V power flow is considered positive. Normally the battery voltage taken is between 320V-390V. Initially the battery SOC is 20%. The nominal battery voltage is 365V and battery current is 3.8A which makes the charging power equal to $365V \times 3.8A = 1440$ VA. Figure 7 represents the source voltage for 1.44kVA charger. The RMS source voltage is 120V and its peak value is 170V. The simulation of the charger is done for 3 seconds. The RMS charging current is 12A.

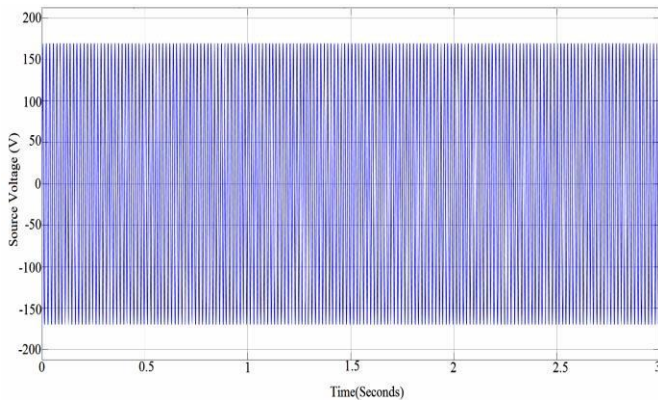


Figure 7: Source Voltage for 1.44kVA Charger.

Figure 8 represents the battery charging current. Its value is 3.8A

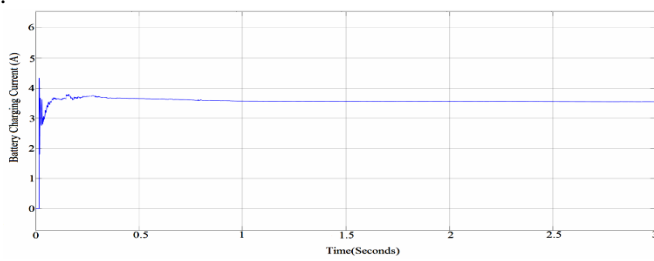


Figure 8: Battery Charging Current for 1.44kVA Charger.

Figure 9 shows the dc link voltage for 1.44kVA charger. The ac input supply is boosted up with the help of boost converter to maintain the dc link voltage near about 390V. The battery nominal voltage is 365V. The ac supply is boosted up so that the current can be conveyed from dc link capacitor to the EV battery for charging purpose.

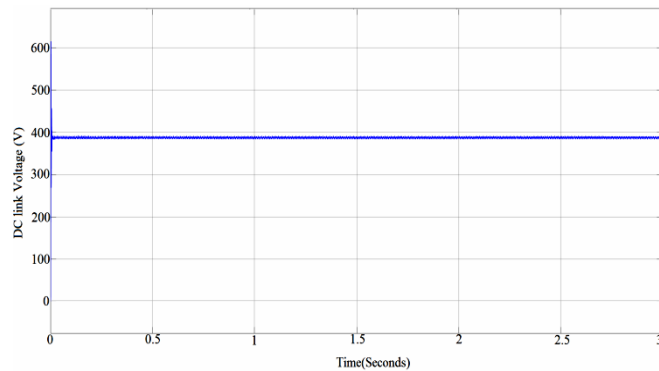


Figure 9: DC Link Voltage for 1.44kVA Charger.

Figure 10 shows the SOC of the battery. Out of two chargers the 6.6kVA charger is swiftest. The 6.6kVA charger takes approximately one-fourth time against 1.44kVA charger to charge the battery.

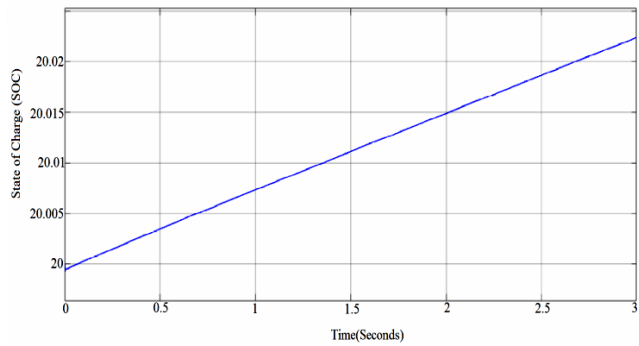


Figure 10: State of Charge (SOC) for 1.44kVA Charger.

6.6kVA Charger

This kind of charger also falls in the category of Level-2 charging system. Figure 11 represents the source voltage for 6.6kVA charger. The RMS value of source voltage is 230V and its peak value is 310V.

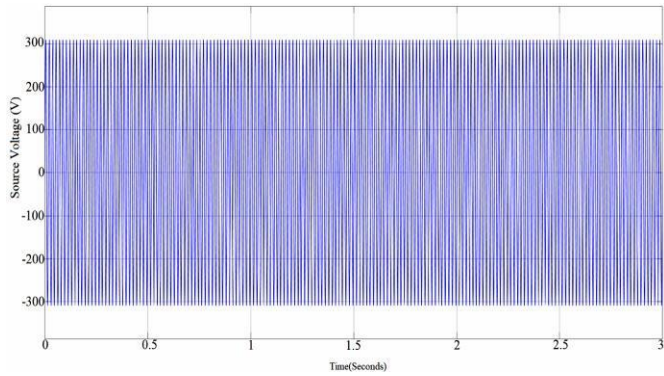


Figure 11: Source Voltage for 6.6kVA Charger.

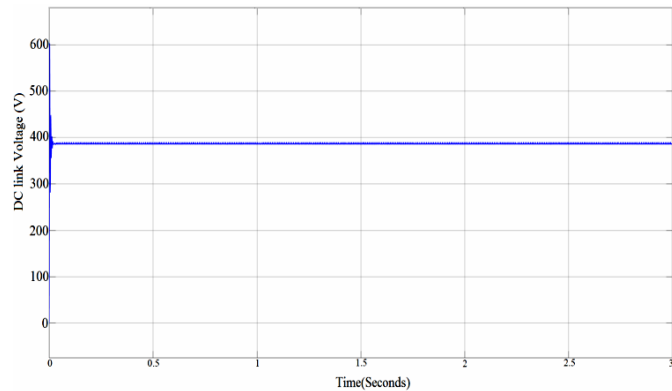


Figure 12: DC link Voltage for 6.6kVA Charger.

Figure 12 and Figure 13 represent the dc link voltage and battery charging current respectively. The RMS value of Battery charging current is 18A. The nominal battery voltage is 365V.

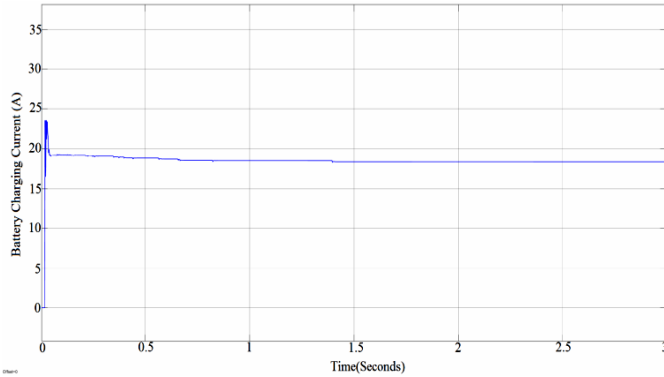


Figure 13: Battery Charging Current for 6.6kVA Charger.

Figure 14 represents the state of charge of the battery for 6.6kVA charger.

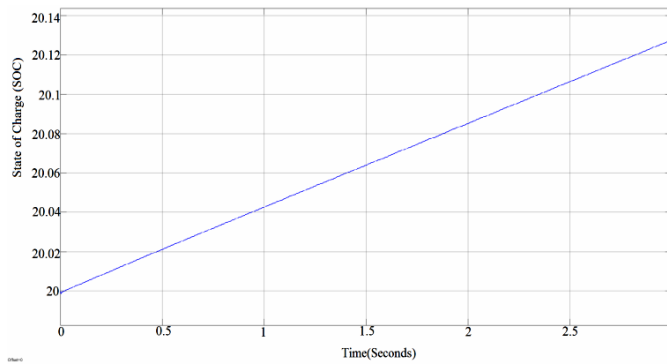


Figure 14: State of Charge (SOC) for 6.6kVA Charger.

The SOC waveform shows that the 6.6kVA charger is fast as compared to 1.44kVA charger. Table IV portrays the comparison between three types of chargers.

Table 4: Comparison of Three Types of Charger

	Level-1 1.44kVA Charger	Level-2 6.6kVA Charger
Supply Voltage	120V RMS	230V RMS
Line Current	12A RMS	24A RMS
DC link Voltage	385V	390V
Battery charging current	3.8A	18A

6. CONCLUSIONS

This work mainly concentrates on the charging of the electric vehicles through single phase PEV transformerless charger. The two controllers used in this charger is used to regulate the battery charging current. The change in P_{cmd} and Q_{cmd} yields the changes in battery charging current (i_{bt}). There are two types of chargers used i.e. i) Level-1 1.44kVA charger ii) Level-2 6.6kVA charger. The outputs of these chargers are shown in Figure 7 to Figure 14 in section IV. The Table III shown above represents the values used in controller for controlling the charging of the electric vehicle battery. The simulation result shows the comparison of three types of chargers in terms of fast and efficient charging. Table V also represents the comparison between various types of controllers. The simulation results show that 6.6kVA charger is much faster than

1.44kVA charger which is better result compared to [11].

REFERENCES

1. M. C. Kisacikoglu, A. Bedir, B. Ozpineci, and L. M. Tolbert, "PHEV-EV charger technology assessment with an emphasis on V2G operation," *OakRidge Nat. Lab., Oak Ridge, TN, USA, Tech. Rep. ORNL/TM-2010/221, Mar. 2012*.
2. Z. Luo, Z. Hu, Y. Song, Z. Xu, and H. Lu, "Optimal coordination of plug-in electric vehicles in power grids with cost-benefit analysis part I: Enabling techniques," *IEEE Trans. Power Systems*, vol. 28, no. 4, pp. 3546–3555, Nov. 2013.
3. D. Manzett *et al.*, "The grid of the future: Ten trends that will shape the grid over the next decade," *IEEE Power Energy Mag.*, vol. 12, no. 3, pp. 26–36, May 2014.
4. M. C. Kisacikoglu, B. Ozpineci, and L. M. Tolbert, "EV/PHEV bidirectional charger assessment for V2G reactive power operation," *IEEE Trans. Power Electron.*, vol. 28, no. 12, pp. 5717–5727, Dec. 2013.
5. M. Kuss, T. Markel, and W. Kramer, "Application of distribution transformer thermal life models to electrified vehicle charging loads using monte-carlo method," in *Elect. Vehicle Symp, Shenzhen, China, Nov. 5–9 2010*.
6. R. Moghe, F. Kreikebaum, J. E. Hernandez, R. P. Kandula, and D. Divan, "Mitigating distribution transformer lifetime degradation caused by grid-enabled vehicle (GEV) charging," *IEEE Energy Conversion Congr. Expo. (ECCE), Phoenix, AZ, 2011*, pp. 835–842.
7. T. S. Bryden, A. J. Cruden, G. Hilton, B. H. Dimitrov, C. P. de León, and Mortimer, "Off-vehicle energy store selection for high rate ev charging station," *6th Hybrid and Electric Vehicles Conference (HEVC 2016)*, pp. 1–9, Nov 2016.
8. K. Mets, T. Verschueren, F. D. Turck, and C. Develder, "Exploiting V2G to optimize residential energy consumption with electrical vehicle (dis)charging," *IEEE First International Workshop on Smart Grid Modeling and Simulation (SGMS)*, pp. 7–12 Oct 2011.
9. H. Liu, Z. Hu, Y. Song, and J. Lin, "Decentralized vehicle-to-grid control for primary frequency regulation considering charging demands," *IEEE Transactions on Power Systems*, vol. 28, no. 3, pp. 3480–3489, Aug 2013.
10. S. Vandoel, T. Holvoet, G. Deconinck, S. Kamboj, and W. Kempton, "A comparison of two given mechanisms for providing ancillary services at the university of delaware," *IEEE International Conference on Smart Grid Communications (Smart Grid - Comm)*, pp. 211–216, Oct 2013.
11. Kisacikoglu, Mithat C., Metin Kesler, and Leon M. Tolbert. "Single phase on-board bidirectional PEV charger for V2G reactive power operation." *IEEE Transactions on Smart Grid*, vol. 6, no. 2, pp. 767-775, 2015.
12. J. G. Pinto, V. Monteiro, H. Goncalves, and J. L. Afonso, "On-board reconfigurable battery charger for electric vehicles with traction-to-auxiliary model," *IEEE Trans. Vehicle Technology*, vol. 63, no. 3, pp. 1104–1116, Mar. 2014.
13. T. Tanaka, T. Sekiya, H. Tanaka, M. Okamoto, and E. Hiraki, "Smart charger for electric vehicles with power-quality compensator on single phase three-wire distribution feeders," *IEEE Trans. Ind. Appl.*, vol. 49, no. 6, pp. 2628–2635, Nov./Dec. 2013.
14. K.-W. Hu and C.-M. Liaw, "On a bidirectional adapter with G2B charging and B2X emergency discharging functions," *IEEE Trans. Ind. Electron.*, vol. 61, no. 1, pp. 243–257, Jan. 2014.
15. A. Arancibia, K. Strunz, and F. Mancilla-David, "A unified single and three-phase control for grid connected electric vehicles," *IEEE Trans. Smart Grid*, vol. 4, no. 4, pp. 1–11, Dec. 2013.
16. "Nissan Leaf Electric Car," 2016. [Online]. Available: <https://www.nissanusa.com/electric-cars/leaf>.

17. M. C. Kisacikoglu, B. Ozpineci, and L. M. Tolbert, "Examination of a PHEV bidirectional charger for V2G reactive power compensation," in Proc. IEEE Appl. Power Electron. Conf. Expo. (APEC), Palm Springs, CA, USA, pp. 458–465, Feb. 2010.
18. R. Teodorescu, F. Blaabjerg, M. Liserre, and P. C. Loh, "Proportional- resonant controllers and filters for grid-connected voltage-sourceconverters," IEE Proceedings - Electric Power Applications, vol. 153, no.5, pp. 750–762, September 2006.
19. A. Timbus, M. Liserre, R. Teodorescu, P. Rodriguez, and F. Blaabjerg, "Evaluation of current controllers for distributed power generation systems," IEEE Transactions on Power Electronics, vol. 24, no. 3, pp. 654–664, March 2009.
20. H. Akagi, Y. Kanazawa, and A. Nabae, "Instantaneous reactive power compensators comprising switching devices without energy storage components," IEEE Transactions on Industry Applications, vol. IA-20, no. 3, pp. 625–630, May 1984.
21. Vijayanand, Y., et al. "New Multilevel Cascaded PWM Inverter Topology for Hybrid Electric Vehicle Drive." International Journal of Electrical and Electronics Engineering (IJEEE) 2.2: 27-40.
22. Upadhyay, Chetan, and Hina Chandwani. "Ultracapacitor–Future of Regenerative Storage in Electric Vehicle." International Journal of Electrical and Electronics Engineering (IJEEE), 2 (2) 41 (2013) 48 (2013).
23. Zabbar, Md Ajijul Bin, and Chisty Nafiz Ahmed. "Design & Implementation of an Unmanned Ground Vehicle (UGV) Surveillance Robot." International Journal of Electrical and Electronics Engineering (IJEEE) 5.6 (2016): 2278-9944.